Inorg. Chem. **2008**, *47*, 8788−8797

Inorganic Chemistry
Article

Formation of Intramolecular Rings in Ferramonocarbollide Complexes

Andreas Franken, Bruce E. Hodson, Thomas D. McGrath, and F. Gordon A. Stone*

Department of Chemistry & Biochemistry, Baylor University, Waco, Texas 76798-7348

Received April 29, 2008

Addition of PPh_2Cl and $Tl[PF_6]$ to CH_2Cl_2 solutions of $[N(PPh_3)_2][6,6,6\text{-}(CO)_3\text{-}closo\text{-}6,1\text{-}FeCB_8H_9]$ (**1**) affords the isomeric *B*-substituted species $[6,6,6\text{-}(CO)_3\text{-}n\text{-}(PHPh_2)\text{-}closo\text{-}6,1\text{-}FeCB_8H_8]$ [$n = 7$ (**2a**) or 10 (**2b**)]. Deprotonation (NaH) of the phosphine ligand in **2a**, with subsequent addition of $[IrCl(CO)(PPh_3)_2]$ and $Tl[PF_6]$, yields the neutral, zwitterionic complex $[6,6,6\text{-}(CO)_3\text{-}4,7\text{-}\mu\text{-}\{Ir(H)(CO)(PPh_3)_2PPh_2\}\text{-}closo\text{-}6,1\text{-}FeCB_8H_7]$ (**3**), which contains a B−P−Ir−B ring. Alternatively, deprotonation using NEt_3, followed by addition of $HC{\equiv}CCH_2Br$, affords $[6,6,6\text{-}(CO)_3\text{-}7\text{-}(PPh_2C{\equiv}CMe)\text{-}closo\text{-}6,1\text{-}FeCB_8H_8]$ (**4**). Addition of $[Co_2(CO)_8]$ to CH_2Cl_2 solutions of the latter gives $[6,6,6\text{-}(CO)_3\text{-}7\text{-}(PPh_2\text{-}\{(\mu\text{-}\eta^2\text{:}\eta^2\text{-}C{\equiv}CMe)Co_2(CO)_6\})\text{-}closo\text{-}6,1\text{-}FeCB_8H_8]$ (**5**), which contains a $\{C_2Co_2\}$ tetrahedron. In the absence of added substrates, deprotonation of the $PHPh_2$ group in compounds **2**, followed by reaction of the resulting anions with CH_2Cl_2 solvent, affords $[6,6,6\text{-}(CO)_3\text{-}n\text{-}(PPh_2CH_2Cl)\text{-}closo\text{-}6,1\text{-}FeCB_8H_8]$ [$n = 7$ (**6a**) or 10 (**6b**)] plus $[6,6\text{-}(CO)_2\text{-}6,7\text{-}\mu\text{-}\{PPh_2CH_2PPh_2\}\text{-}closo\text{-}6,1\text{-}FeCB_8H_8]$ (**7**, formed from **2a**), of which the latter species possesses an intramolecular B−P−C−P−Fe ring. Addition of Me_3NO to CH_2Cl_2 solutions of **2a** causes loss of an Fe-bound CO ligand and formation of $[6,6\text{-}(CO)_2\text{-}6,7\text{-}\mu\text{-}\{NMe_2CH_2PPh_2\}\text{-}closo\text{-}6,1\text{-}FeCB_8H_8]$ (**8**), which incorporates a B−P−C−N−Fe ring. A similar reaction in the presence of ligands L yields $[6,6\text{-}(CO)_2\text{-}6\text{-}L\text{-}7\text{-}(PPh_2CH_2Cl)\text{-}closo\text{-}6,1\text{-}FeCB_8H_8]$ [L = PEt_3 (**9**) or $CNBu^t$ (**10**)], in addition to **8**.

Introduction

In recent times numerous transition metal half-sandwich metallamonocarbollide compounds have been described with a metal atom incorporated in a cage framework containing 12 or fewer vertices. Our initial studies focused on those species with 12-atom, icosahedral frameworks.[1] These complexes were usually obtained by treating salts of the long known[2] monoanion $[nido\text{-}7\text{-}CB_{10}H_{13}]^-$ with suitable transition element reagents. Thus reaction of this carborane anion with $[Fe_3(CO)_{12}]$ affords $[2,2,2\text{-}(CO)_3\text{-}closo\text{-}2,1\text{-}FeCB_{10}H_{11}]^-$,[3] a species isolobal with $[Mn(CO)_3(\eta\text{-}C_5H_5)]$. As reports of straightforward syntheses of monocarbon carboranes with fewer than 10 boron atoms (e.g., salts of $[arachno\text{-}9\text{-}CB_9H_{14}]^-$, $[6\text{-}Ph\text{-}nido\text{-}6\text{-}CB_9H_{11}]^-$, $[closo\text{-}1\text{-}CB_8H_9]^-$, and $[closo\text{-}1\text{-}CB_7H_8]^-$) have appeared,[4] we have been able to extend very considerably the scope of our studies of reactions of metallamonocarbollide compounds, generally obtaining products with unusual molecular structures.

Not unexpectedly the chemical reactivity of these new metal complexes varies according to the transition element they contain, for example, iron versus manganese, and with the metal's oxidation state. However, an especially interesting feature of the chemistry is the discovery that in several of the new compounds initially formed the terminal {B−H} groups can react further, affording molecules with functional organic groups attached to the peripheral boron atoms.[1,5] These products may in turn be converted into other new molecules in which the *closo*-cage may or may not play a role. The functionalization of (hetero)borane cages has been of interest for many years, particularly with a view to medical

* To whom correspondence should be addressed. E-mail: gordon_stone@baylor.edu.

(1) McGrath, T. D.; Stone, F. G. A. *Adv. Organomet. Chem.* **2005**, *53*, 1.
(2) Noth, W. H.; Little, J. L.; Lawrence, J. R.; Scholer, F. R.; Todd, L. J. *Inorg. Synth.* **1968**, *11*, 33.
(3) Ellis, D. D.; Franken, A.; Jelliss, P. A.; Stone, F. G. A.; Yu, P.-Y. *Organometallics* **2000**, *19*, 1993.
(4) (a) Brellochs, B. In *Contemporary Boron Chemistry*; Davidson, M. G., Hughes, A. K., Marder, T. B., Wade, K.; Royal Society of Chemistry: Cambridge, U.K., 2000, p 212. (b) Brellochs, B.; Backovsky, J.; Stibr, B.; Jelinek, T.; Holub, J.; Bakardjiev, M.; Hnyk, D.; Hofmann, M.; Cisarova, I.; Wrackmeyer, B. *Eur. J. Inorg. Chem.* **2004**, 3605.
(5) See also Jelliss, P. A.; Stone, F. G. A. *J. Organomet. Chem.* **1995**, *500*, 307.

10.1021/ic800780w CCC: $40.75
Published on Web 09/04/2008

Chart 1

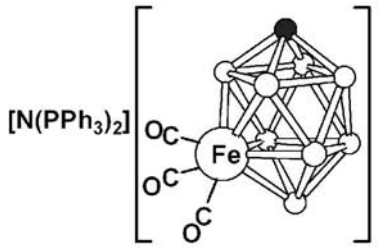

1

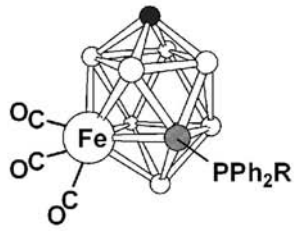

R	
2a	H
4	C≡CMe
5	$CCo_2(CO)_6CMe$
6a	CH_2Cl

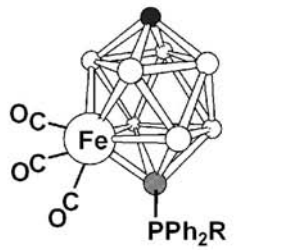

R	
2b	H
6b	CH_2Cl

applications; thus the *in vivo* solubility of boron-containing clusters is one of the essential factors for effective Boron Neutron Capture Therapy (BNCT).[6]

Complexes obtained from iron carbonyls and $\{CB_7\}$ or $\{CB_8\}$ precursors[7,8] appear readily to yield molecules that display interesting derivative chemistry.[9] In this paper we focus on compounds derived from the anion $[6,6,6\text{-}(CO)_3\text{-}closo\text{-}6,1\text{-}FeCB_8H_9]^-$,[8] here used as the $[N(PPh_3)_2]^+$ salt (**1**; see Chart 1), in which the introduction of cage substituents is readily accomplished. Thus, a {B−H} substitution reaction yields a neutral, zwitterionic species containing a {B−$PHPh_2$} vertex. Few examples of clusters involving this unit have been reported,[10] and derivatization of this compound affords several novel and surprising products.

Results and Discussion

Addition of PPh_2Cl and $Tl[PF_6]$ to CH_2Cl_2 solutions of the ferramonocarbollide complex $[N(PPh_3)_2][6,6,6\text{-}(CO)_3\text{-}closo\text{-}6,1\text{-}FeCB_8H_9]$ (**1**)[8] affords two neutral, zwitterionic, isomeric species $[6,6,6\text{-}(CO)_3\text{-}n\text{-}(PHPh_2)\text{-}closo\text{-}6,1\text{-}FeCB_8H_8]$ [$n = 7$ (**2a**) or 10 (**2b**)] in the approximate ratio 49:1 (Chart 1). Attempts to separate completely these compounds by column chromatography proved unsuccessful, small quantities of **2b** appearing in all samples of **2a**. However, full characterization of the latter was achieved. Physical and spectroscopic data for **2a** and **2b** (where possible) are presented in Tables 1−3. The IR spectrum of **2a** contains strong CO stretching bands at 2056 and 1995 cm^{-1}, values higher than those for the precursor **1** (2033 and 1964 cm^{-1}), as is to be expected following formation of a neutral species from an anionic complex. An $^{11}B\{^1H\}$ NMR study revealed six signals for **2a** in intensity ratio 1:1:2(1+1 coincidence): 1:2(1+1 coincidence):1 (low to high field), indicating a lack of symmetry in the cluster. The highest field, doublet resonance (δ −31.9) retained this multiplicity in the corresponding ^{11}B spectrum and as such was assigned to the {B−$PHPh_2$} vertex. The phosphorus atom of this unit gave rise to a quartet resonance in the $^{31}P\{^1H\}$ NMR spectrum at δ 1.5 [$J(BP) = 128$ Hz] and to a doublet-of-quartets peak [$J(HP) = 433$ Hz] in the ^{31}P NMR spectrum. Additionally, the phosphorus-bound hydrogen atom appeared in the ^1H NMR spectrum as a doublet peak [$J(PH) = 426$ Hz] centered on δ 6.32, which collapsed into a singlet upon ^{31}P decoupling. The ^1H NMR spectrum also contained a broad resonance due to the cage {CH} unit at δ 5.21 with complex multiplet resonances in the range δ 7.77−7.31 due to the Ph groups in the molecule. The $^{13}C\{^1H\}$ spectrum of **2a** revealed resonances due to the Fe-bound CO ligands at δ 210.2 and to the cage carbon atom at δ 60.5.

Attempts to isolate significant quantities of **2b** proved unsuccessful as a consequence of its low yield and physical properties similar to those of its isomer **2a**. In the reactions involving **2a** discussed below, small quantities of **2b** are assumed to be present. The paucity of data for **2b** prevents any complete, even tentative characterization. However, examination of $^{11}B\{^1H\}$ and $^{31}P\{^1H\}$ NMR data of **2a/2b** mixtures, in addition to the crystal structure of **6b** obtained fortuitously and discussed below, fully justifies the formulation for **2b**. Thus, an $^{11}B\{^1H\}$ NMR study of a **2a/2b** mixture reveals a low intensity doublet resonance at δ 48.6, suggesting the presence of a {B−P} unit other than that in **2a**. This δ value is significantly lower field in comparison with

(6) For a recent review, see Bregadze, V. I.; Sivaev, I. B.; Glazun, S. A. *Anti-Cancer Agents Med. Chem.* **2006**, *6*, 75.
(7) Franken, A.; McGrath, T. D.; Stone, F. G. A. *Organometallics* **2005**, *24*, 5157.
(8) Franken, A.; McGrath, T. D.; Stone, F. G. A. *Inorg. Chem.* **2006**, *45*, 2669.
(9) (a) Franken, A.; McGrath, T. D.; Stone, F. G. A. *J. Am. Chem. Soc.* **2006**, *128*, 16169. (b) Franken, A.; Hodson, B. E.; McGrath, T. D.; Stone, F. G. A. *Dalton Trans.* **2007**, 2254.
(10) (a) Fontaine, X. L. R.; Greenwood, N. N.; Kennedy, J. D.; MacKinnon, P.; Thornton-Pett, M. *J. Chem. Soc., Dalton Trans.* **1988**, 2059. (b) Zakharkin, L. I.; Ol'shevskaya, V. A.; Zhigareva, G. G.; Antonovich, V. A.; Petrovskii, P. V.; Yanovskii, A. I.; Polyakov, A. V.; Struchkov, Yu. T. *Metalloorg. Khimi.* **1989**, *2*, 1274. (c) Shea, S. L.; Jelinek, T.; Perera, S. D.; Stibr, B.; Thornton-Pett, M.; Kennedy, J. D. *Inorg. Chim. Acta* **2004**, *357*, 3119.

Table 1. Analytical and Physical Data

compd	color	ν_{max}(CO[a]/cm^{-1}	anal/%[b] C	H
[6,6,6-$(CO)_3$-7-$(PHPh_2)$-*closo*-6,1-$FeCB_8H_8$] (**2a**)[c]	yellow	2056 s, 1995 s	(44.4) 44.2	(4.4) 4.1
[6,6,6-$(CO)_3$-4,7-μ-{Ir(H)(CO)$(PPh_3)_2PPh_2$}-*closo*-6,1-$FeCB_8H_7$] (**3**)	yellow	2041 s, 1981 s	(54.1) 53.8	(4.1) 4.3
[6,6,6-$(CO)_3$-7-$(PPh_2C{\equiv}CMe)$-*closo*-6,1-$FeCB_8H_8$] (**4**)	yellow	2054 s, 1995 s	(48.5) 48.3	(4.5) 4.7
[6,6,6-$(CO)_3$-7-$(PPh_2\{(\mu\text{-}\eta^2{:}\eta^2\text{-}C{\equiv}CMe)Co_2(CO)_6\})$-*closo*-6,1-$FeCB_8H_8$] (**5**)	red	2099 s, 2068 s, 2054 s, 2038 s, 1994 s	(39.7) 40.1	(2.8) 2.9
[6,6,6-$(CO)_3$-7-(PPh_2CH_2Cl)-*closo*-6,1-$FeCB_8H_8$] (**6a**)[d]	yellow	2056 s, 1999 s	(42.4) 42.2	(4.2) 4.4
[6,6-$(CO)_2$-6,7-μ-{$PPh_2CH_2PPh_2$}-*closo*-6,1-$FeCB_8H_8$] (**7**)	yellow	1994 s, 1948 s	(55.8) 55.6[e]	(5.0) 5.1
[6,6-$(CO)_2$-6,7-μ-{$NMe_2CH_2PPh_2$}-*closo*-6,1-$FeCB_8H_8$] (**8**)	orange	1983 s, 1927 s	(46.8) 46.4	(5.7) 6.1
[6,6-$(CO)_2$-6-PEt_3-7-(PPh_2CH_2Cl)-*closo*-6,1-$FeCB_8H_8$] (**9**)	yellow	1974 s, 1924 s	(46.3) 46.1	(6.2) 6.4
[6,6-$(CO)_2$-6-$CNBu^t$-7-(PPh_2CH_2Cl)-*closo*-6,1-$FeCB_8H_8$] (**10**)	yellow	2004 s, 1960 s	(47.0) 47.3	(5.5) 5.7

[a] Measured in CH_2Cl_2; a broad, medium-intensity band observed at ca. 2500−2550 cm^{-1} in the spectra of all compounds is due to B−H absorptions. In addition: for **4**, ν_{max}(C≡C) 2211 w cm^{-1}; for **10**, ν_{max}(C≡N) 2158 s cm^{-1}. [b] Calculated values are given in parentheses. In addition, % N: for **8**, (3.0) 2.9; for **10**, (2.6) 2.8. [c] Samples contained approximately 2% [6,6,6-$(CO)_3$-10-$(PHPh_2)$-*closo*-6,1-$FeCB_8H_8$] (**2b**). [d] Samples contained approximately 2% [6,6,6-$(CO)_3$-10-(PPh_2CH_2Cl)-*closo*-6,1-$FeCB_8H_8$] (**6b**). [e] Co-crystallizes with one mol. equiv. of CH_2Cl_2.

Table 2. ^{1}H and ^{13}C NMR Data[a]

compd	^{1}H/δ[b]	^{13}C/δ[c]
2a	7.77−7.31 (m, 10H, Ph), 6.32 [d, *J*(PH), 1H, PH = 426], 5.21 (br s, 1H, cage CH)	210.2 (CO), 135.1−128.5 (Ph), 60.5 (br, cage C)
3	7.50−6.98 (m, 40H, Ph), 4.11 (br, 1H, cage CH), −8.68 (br, 1H, Ir−H)	211.8 (Fe−CO), 180.9 (br, Ir−CO), 134.2−128.5 (Ph), 60.5 (br, cage C)
4	7.93−7.53 (m, 10H, Ph), 5.23 (br, 1H, cage CH), 2.11 (s, 3H, Me)	210.4 (CO), 132.0−122.4 (Ph), 114.6 [d, *J*(PC) = 29, P*C*≡C], 66.5 (C≡*C*Me), 59.9 (br, cage C), 5.5 (Me)
5	8.18−7.50 (m, 10H, Ph), 5.12 (br, 1H, cage CH), 3.17 (s, 3H, Me)	209.8 (Fe−CO), 197.5 (Co−CO), 133.8−127.3 (Ph), 106.0 (*C*Me), 72.2 [d, *J*(PC) = 30, PC], 60.9 (br, cage C), 23.5 (Me)
6a	8.14−7.38 (m, 10H, Ph), 5.38 (br, 1H, cage CH), 4.23 [dd, *J*(H_aH_b) = 32, *J*(PH) = 144, 1H, P*CH$_a$*H$_b$], 4.13 [dd, *J*(H_bH_a) = 32, *J*(PH) = 144, 1H, PCH$_a$*H$_b$*]	210.1 (CO), 133.4−128.5 (Ph), 60.8 (br, cage C), 35.8 [d, *J*(PC) = 40, CH_2]
7	7.88−7.21 (m, 20H, Ph), 5.29 (br, 1H, cage CH), 3.66 (m, 1H, CH_2), 3.20 (m, 1H, CH_2)	215.5 [d, *J*(PC) = 21, CO], 212.8 [d, *J*(PC) = 19, CO], 133.7−128.4 (Ph), 60.7 (br, cage C), 36.7 [dd, *J*(PC) = 18 and 54, CH_2]
8	7.77−7.48 (m, 10H, Ph), 5.05 (br s, 1H, cage CH), 3.78 [dd, *J*(PH) = 42, *J*(HH) = 13, 1H, CH_2], 3.15 [dd, *J*(PH) = 15, *J*(HH) = 5, 1H, CH_2], 3.08, 2.22 (s × 2, 3H × 2, Me × 2)	218.2 (CO), 216.4 (CO), 134.0−128.5 (Ph), 68.3 [d, *J*(PC) = 45, NCH_2P], 62.6, 60.3 (NMe × 2), 57.9 (br, cage C)
9	7.59−7.45 (m, 10H, Ph), 5.13 (br s, 1H, cage CH), 4.29 (br, 2H, $BPCH_2$), 1.68 (m, 6H, $FePCH_2$), 1.07 (m, 9H, Me)	219.5 [d, *J*(PC) = 27, CO], 215.1 [d, *J*(PC) = 27, CO], 133.7−128.4 (Ph), 59.1 (br, cage C), 36.0 [d, *J*(PC) = 35, $BPCH_2$], 19.3 [d, *J*(PC) = 29, $FePCH_2$], 7.6 (Me)
10	7.75−7.43 (m, 10H, Ph), 5.18 (br s, 1H, cage CH), 4.17 (m, 2H, CH_2), 1.32 (s, 9H, Me)	215.2 (CO), 213.7 (CO), 156.3 (N≡C), 133.7−121.4 (Ph), 58.5 (br, cage C), 57.6 (*C*Me$_3$), 36.1 [d, *J*(PC) = 39, PCH_2], 30.0 (C*Me$_3$*)

[a] Chemical shifts (δ) in ppm, coupling constants (*J*) in hertz, measurements at ambient temperatures in CD_2Cl_2. [b] Resonances for terminal BH protons occur as broad unresolved signals in the range δ ca. −1 to +3. [c] ^{1}H-decoupled chemical shifts are positive to high frequency of $SiMe_4$.

Table 3. ^{11}B and ^{11}P NMR Data[a]

compd	^{11}B/δ[b]	^{31}P/δ[c]
2a	55.9, −3.4, −3.0 (2B), −23.0, −24.4 (2B), −31.9 [d, *J*(PB) = 127]	1.5 [q, *J*(BP) = 128]
3	53.6, 1.3, −6.5 (2B), −17.5, −23.8 (2B), −34.1	2.3 [d, *J*(PP) = 260, Ir−P], −3.4 (d, Ir−P), −48.3 (br, B−P)
4	54.8, −2.0, −3.2, −5.2, −22.7, −24.2, −25.3, −28.3 [d, *J*(PB) = 120]	1.3 [q, *J*(BP) = 122]
5	54.6, −2.8, −5.2, −23.3 (2B), −25.0 (2B), −27.5 [d, *J*(PB) = 132]	22.4 [q, *J*(BP) = 126]
6a	54.2, −3.6, −5.6 (2B), −22.8, −24.0, −25.0, −30.5 [d, *J*(PB) = 127]	17.5 [q, *J*(BP) = 127]
7	57.5, −0.3, −1.6, −4.2, −22.8, −23.9, −24.5, −26.1 [d, *J*(PB) = 131]	77.4 [d, *J*(PP) = 95], 18.5 [br dq, *J*(BP) = ca. 132]
8	58.8, −0.4, −2.1, −7.1, −23.3 (2B), −24.6, −29.9	23.7 [q, *J*(BP) = 130]
9	52.6, −3.7, −5.6, −6.8, −23.0, −23.9, −24.5, −32.3 [d, *J*(PB) = 122]	59.9 (Fe−P), 19.5 [q, *J*(BP) = 120, B−P]
10	52.5, −5.9 (3B), −22.9, −24.4, −24.6, −32.3 [d, *J*(PB) = 125]	18.7 [q, *J*(BP) = 122]

[a] Chemical shifts (δ) in ppm, coupling constants (*J*) in hertz, measurements at ambient temperatures in CD_2Cl_2. [b] ^{1}H-decoupled chemical shifts are positive to high frequency of $BF_3{\cdot}Et_2O$ (external); resonances are of unit integral except where indicated. In addition, for **2b** δ 48.6 [d, *J*(PB) = 127]; for **6b** δ 49.8 [d, *J*(PB) = 155]. [c] ^{1}H-decoupled chemical shifts are positive to high frequency of 85% H_3PO_4 (external). In addition, for **2b** δ −4.5 [q, *J*(BP) = 74]; for **6b** δ 14.1 [q, *J*(BP) = 155].

the corresponding value for the {B−P} unit in **2a** (δ −31.9), as expected for such a group occupying the four-connectivity position [B(10)], rather than a five-connectivity position as seen in **2a** [B(7)]. The presence of a phosphorus substitutent at B(10) in **6b** (see below) fully corroborates this suggestion. In **2b**, the P atom of the {B−$PHPh_2$} unit appears as a low intensity quartet resonance in the corresponding ^{31}P{^{1}H} NMR spectrum at δ −4.5. Unfortunately, further definitive assignment of any NMR data for **2b** was not possible.

The mechanism of formation of **2a** (and **2b**) is believed to involve initial reaction between PPh_2Cl and $Tl[PF_6]$ to generate $\{PPh_2\}^+$. This species then abstracts a hydride from a {B−H} unit in **1**, forming $PHPh_2$ and a "denuded", formally positively charged boron vertex. Attack at this "naked" site by the diphenylphosphine molecule is then reasonable. The preferential formation of the B(7)- (**2a**) rather than B(10)-substituted product (**2b**) is intuitively associated with the hydrogen atom of the {B(7)H} vertex in **1** being more hydridic.

Deprotonation of the {B−P*H*Ph_2} fragment in **2a** is facile using a variety of bases; the resulting species, which contains an electron rich phosphorus atom, readily reacts with electrophiles. Thus, reaction of **2a** with excess NaH, followed by filtration and addition to the filtrate of $[IrCl(CO)(PPh_3)_2]$

Chart 2

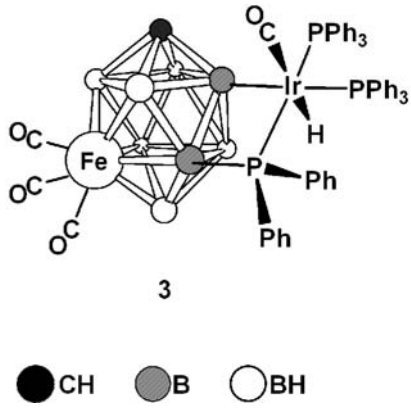

and $Tl[PF_6]$ (a source of the $\{Ir(CO)(PPh_3)_2\}^+$ fragment) affords the zwitterionic compound [6,6,6-$(CO)_3$-4,7-μ-$\{Ir(H)(CO)(PPh_3)_2PPh_2\}$-*closo*-6,1-$FeCB_8H_7$] (**3**) (Chart 2). An $^{11}B\{^1H\}$ NMR study of **3** revealed the asymmetric nature of the cluster with six peaks in the intensity ratios 1:1:2:1:2:1. The signals were broad, and as a result the expected doublet resonance corresponding to the {*B*−P} vertex was not identified. Similarly, the ^{11}B NMR spectrum failed to provide any information regarding coupling to exopolyhedral atoms at each vertex, even under variable temperature conditions (233 to 313 K). The resonance due to the {*B*−Ir} unit, which would be expected to have singlet multiplicity in this spectrum, was therefore not identified. Strong CO stretching bands appeared in the IR spectrum of **3** at 2041 and 1981 cm^{-1}, with corresponding resonances in the $^{13}C\{^1H\}$ NMR spectrum at δ 211.8 (Fe−CO) and 180.9 (Ir−CO), respectively. The latter signal suffered from significant broadening because of unresolved coupling with the Ir-bound phosphorus ligands. A ^1H NMR spectrum of **3** contained complex multiplet peaks in the range δ 7.50−6.98 due to the phenyl groups, as well as two broad peaks at δ 4.11 and δ −8.68 assigned to the cage {CH} and {Ir−H} units, respectively. The $^{31}P\{^1H\}$ NMR spectrum contained a very broad resonance at δ −48.3 for the {B−P} unit, in addition to broad doublet peaks assigned to PPh_3 groups at δ 2.3 and −3.4. Both the $^{31}P\{^1H\}$ and ^1H NMR spectra indicated the presence of small quantities of as yet unidentified impurities.

The molecular structure of compound **3** determined by X-ray diffraction is displayed in Figure 1. Its iridium atom [Ir(1)] coordinates to B(4) and to the phosphorus atom of the {B(7)−P(1)} unit, forming a four-membered B−P−Ir−B ring. The bridged B(4)−B(7) connectivity [1.814(7) Å] is comparable with the remaining B−B distances within the cluster (average 1.820 Å). The B(7)−B(4)−Ir(1)−P(1) ring is distorted into a shallow butterfly configuration, the triangles defined by B(4)B(7)P(1) and P(1)Ir(1)B(4) being tilted by 5.8° relative to one another. Internal angles at each corner are 102.0(3) [B(4)], 71.91(13) [Ir(1)], 92.66(16) [P(1)], and 93.1(3)° [B(7)]. This deviation from planarity is assumed to be due both to the differing atomic radii of the ring constituents, particularly the large iridium atom, and to steric interactions between phenyl rings on the peripheral phosphine

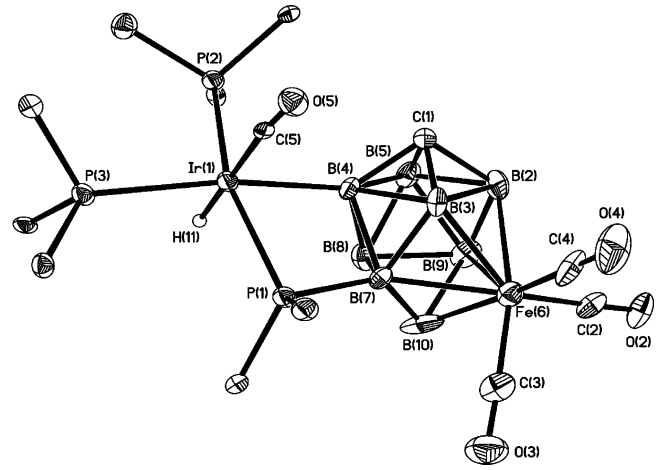

Figure 1. Structure of **3** showing the crystallographic labeling scheme. In this and subsequent figures, thermal ellipsoids are draw with 40% probability. For clarity, only the ipso carbon atoms of phenyl rings, and only chemically significant H atoms, are shown. Selected distances (Å) and angles (deg) are as follows: Ir(1)−B(4) 2.198(6), B(4)−B(7) 1.818(9), P(1)−B(7) 1.920(7), Ir(1)−P(1) 2.3985(13), Ir(1)−H(11) 1.67(2), Ir(1)−C(5) 1.928(6), Ir(1)−P(2) 2.3513(14), Ir(1)−P(3) 2.4213(15), Fe(6)−B(2) 2.210(7), Fe(3)−B(3) 2.218(7), Fe(6)−B(7) 2.222(7), Fe(6)−B(9) 2.208(7), Fe(6)−B(10) 2.028(8); B(4)−Ir(1)−P(1) 71.88(16), B(7)−P(1)−Ir(1) 92.69(19), B(7)−B(4)−Ir(1) 102.5(4), B(4)−B(7)−P(1) 92.6(4).

groups. The iridium center has acquired a hydride ligand, presumably sourced from the {B(4)−H} vertex in **2a**. Formation of the ring moiety in **3** presumably proceeds via initial coordination of the $\{Ir(CO)(PPh_3)_2\}^+$ fragment at the phosphorus atom of the $\{B-PPh_2\}^-$ unit, followed by oxidative insertion of the iridium atom into the adjacent exopolyhedral B(4)−H bond.

Deprotonation of **2a** using NEt_3, followed by addition of $HC{\equiv}CCH_2Br$, affords [6,6,6-$(CO)_3$-7-($PPh_2C{\equiv}CMe$)-*closo*-6,1-$FeCB_8H_8$] (**4**) (Chart 1). Inseparable minor impurities present in samples of **4** are attributed to the intuitive initial product containing a $\{PPh_2CH_2C{\equiv}CH\}$ unit and to small quantities of the corresponding B(10)-substituted isomers formed from **2b**. Unfortunately, none of these other species could be isolated in sufficient quantity to allow full identification. The observed redistribution of hydrogen atoms in the $\{PPh_2C{\equiv}CMe\}$ group in the final product **4** may depend upon the presence of the nearby, formally positively charged phosphorus atom. In any event, such terminal-to-internal rearrangements for alkynes are well-known and in the present case might be catalyzed by the weak base NEt_3.[11]

The ^1H NMR spectrum of **4** contains peaks assigned to the phosphine-bound Ph groups and to the cage {CH} units at δ 7.93−7.53 and δ 5.23, respectively, and the $\{PC{\equiv}CMe\}$ methyl protons gave rise to a singlet resonance at δ 2.11. In the $^{13}C\{^1H\}$ NMR study, corresponding peaks due to the $\{PC{\equiv}CMe\}$ fragment were observed at δ 114.6 [d, J(PC) = 29 Hz], 66.5, and 5.5, corresponding to the P*C*≡, *C*Me, and Me groups, respectively. Also contained therein were peaks due to the Fe-bound CO ligands (δ 210.4), cage {CH} unit (δ 59.9), and Ph groups (δ 132.0−122.4). The carbonyl ligands were observed in the IR spectrum of **4** as strong

(11) Smith, M. B.; March, J. In *Advanced Organic Chemistry*; John Wiley and Sons: Hoboken, NY, 2007; pp 768−769.

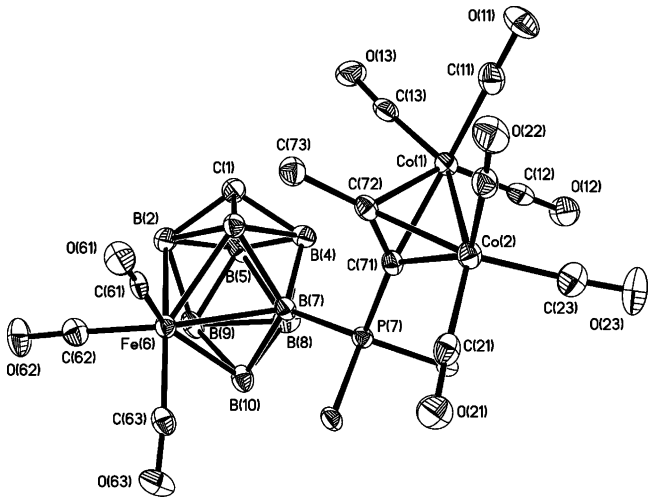

Figure 2. Structure of **5** showing the crystallographic labeling scheme. Selected distances (Å) are as follows: B(7)−P(7) 1.935(4), P(7)−C(71) 1.781(3), C(71)−C(72) 1.347(3), C(72)−C(73) 1.490(3), C(71)−Co(1) 1.951(3), C(71)−Co(2) 1.994(3), C(72)−Co(1) 1.971(3), C(72)−Co(2) 1.960(3), Fe(6)−B(2) 2.228(4), Fe(6)−B(3) 2.217(3), Fe(6)−B(7) 2.223(3), Fe(6)−B(9) 2.205(3), Fe(6)−B(10) 2.043(3).

absorptions at 2054 and 1995 cm^{-1}, as was a weak C≡C stretch at 2211 cm^{-1}. The asymmetric nature of the carborane cage fragment was revealed by the presence of eight peaks of unit intensity in the $^{11}B\{^1H\}$ NMR study. The lowest field resonance in the latter spectrum (δ −28.3) appeared as a doublet and hence was assigned to the {B−P} vertex; this unit also gave rise to a quartet peak at δ 1.3 [J(BP) = 122 Hz] in the $^{31}P\{^1H\}$ NMR spectrum.

Addition of $[Co_2(CO)_8]$ to CH_2Cl_2 solutions of **4** gives [6,6,6-$(CO)_3$-7-(PPh_2-{(μ-η^2:η^2-C≡CMe)$Co_2(CO)_6$})-*closo*-6,1-$FeCB_8H_8$] (**5**) (Chart 1), in which a $\{Co_2(CO)_6\}$ fragment orthogonally bridges the triple bond of the pendant {PC≡CMe} group in **4**, forming a $\{C_2Co_2\}$ tetrahedron. Similar reactivity of pendant acetylene groups has been observed in other subicosahedral dicarborane species.[12] An IR spectrum of **5** revealed strong CO stretching frequencies at 2099, 2068, 2054, 2038, and 1994 cm^{-1}. Peaks due to these groups were observed at δ 209.8 and 197.5 (Fe−CO and Co−CO, respectively) in the $^{13}C\{^1H\}$ NMR spectrum of **5**, as were resonances assigned to the {PC≡CMe} fragment [δ 106.0 (*C*Me), 72.2 [d, J(PC) = 30 Hz, P*C*], and 23.5 (Me)], and to the cage carbon atom (δ 60.9). A ^1H NMR spectrum revealed resonances due to the cage {CH} unit and the methyl group at δ 5.12 and δ 3.17, respectively. As in **2a**, **3**, and **4**, the presence of the pendant {PC≡CMe} moiety in **5** renders the cluster asymmetric, and hence the $^{11}B\{^1H\}$ NMR spectrum contained six peaks with relative intensity 1:1:1:2:2:1 (low to high field), of which the highest field peak (δ −27.5) appeared as a doublet [J(PB) = 132 Hz], and hence was assigned to the {B−P} vertex.

The structure of **5** was fully established by an X-ray diffraction study (Figure 2). The atomic arrangement in the $\{FeCB_8\}$ unit remains unchanged in comparison with **4**, and the B(2)−B(3) connectivity is slightly elongated [1.968(5) Å] in comparison with average B−B distances (1.800 Å) in the remainder of the cluster. Average C−B and Fe−B distances are 1.594 and 2.183 Å, respectively. The $\{C_2Co_2\}$ unit, typically, describes a closed tetrahedron and the {PPh_2C{μ-$Co_2(CO)_6$}CMe} fragment as a whole is oriented to provide the least possible steric interaction with the Fe-bound CO ligands. This structure is in agreement with the formulation of **4** as also containing a pendant {PC≡CMe} fragment.

Addition of NEt_3 to CH_2Cl_2 solutions of **2a** (containing small amounts of its isomer **2b** as noted above) afforded three identifiable species: the two isomeric molecules [6,6,6-$(CO)_3$-*n*-(PPh_2CH_2Cl)-*closo*-6,1-$FeCB_8H_8$] [*n* = 7 (**6a**) or 10 (**6b**)] (Chart 1), with the latter produced in very small quantities, in addition to the "ring"-containing compound [6,6-$(CO)_2$-6,7-μ-{$PPh_2CH_2PPh_2$}-*closo*-6,1-$FeCB_8H_8$] (**7**) (Scheme 1). As with **2b** above, bulk compound **6b** was not itself isolated but fortuitously was characterized by a crystallographic determination (discussed below), along with limited supporting NMR data. The formation of **6a** and **6b** is assumed to proceed via initial deprotonation of the {$PHPh_2$} group in **2a** or **2b**, respectively. In the absence of other suitable substrates, the intermediates formed react directly with CH_2Cl_2 solvent molecules by simple nucleophilic Cl displacement.

An IR spectrum of **6a** displayed strong CO group absorptions at 2056 and 1999 cm^{-1}, almost identical to those for **2a** (2056 and 1995 cm^{-1}). The $^{11}B\{^1H\}$ NMR spectrum for **6a** likewise indicates its carborane moiety to be electronically similar to that for **2a**, with the lowest field peak (δ −30.5) appearing as a doublet [J(PB) = 127 Hz], because of the exopolyhedral {PPh_2CH_2Cl} group; the corresponding signal for the {$PHPh_2$} group in **2a** appears at δ −31.9. A resonance assigned to the carbonyl ligands in **6a** appeared in its $^{13}C\{^1H\}$ NMR spectrum at δ 210.1, as were peaks due to the cage carbon atom (δ 60.8) and to the {PPh_2CH_2Cl} group methylene carbon [δ 35.8, d, J(PC) = 40 Hz]. The two protons of the latter group appeared in the ^1H NMR spectrum as separate doublet-of-doublet resonances at δ 4.13 and 4.23 [$J(H_aH_b)$ = 32 Hz; J(PH) = 144 Hz in each case]. The phosphorus atom of the {B−P} vertex was observed as a quartet resonance in the $^{31}P\{^1H\}$ NMR spectrum at δ 17.5 [J(BP) = 127 Hz].

Evidence for [6,6,6-$(CO)_3$-10-(PPh_2CH_2Cl)-*closo*-6,1-$FeCB_8H_8$] (**6b**) was provided in the form of a low-field doublet resonance in the $^{11}B\{^1H\}$ NMR spectrum at δ 49.8, analogous to that for **2b**, and a quartet resonance at δ 14.1 in the $^{31}P\{^1H\}$ NMR spectrum. A comparison of relative peak integrals indicates an approximate 49:1 ratio (**6a**:**6b**) in the product mixture. Single crystal X-ray diffraction quality crystals were grown by slow diffusion of petroleum ether and a CH_2Cl_2 solution of a **6a**/**6b** mixture and led to the structural analysis of both **6a** (included as Supporting Information) and **6b** (see Figure 3). Within the molecule shown, the central $\{FeCB_8\}$ cluster core carries an exopolyhedral {PPh_2CH_2Cl} unit at the four connected B(10) vertex. As a result, a mirror plane is present within the molecule, inconsistent with the $^{11}B\{^1H\}$ NMR data obtained for **6a**.

(12) (a) Nie, Y.; Goswami, A.; Siebert, W. *Z. Naturforsch., B* **2005**, *60*, 597. (b) Franken, A.; McGrath, T. D.; Stone, F. G. A. *Organometallics* **2008**, *27*, 908.

Scheme 1. Formation and Interconversion of Compounds **6a** and **7**−**10** from **2a**[a]

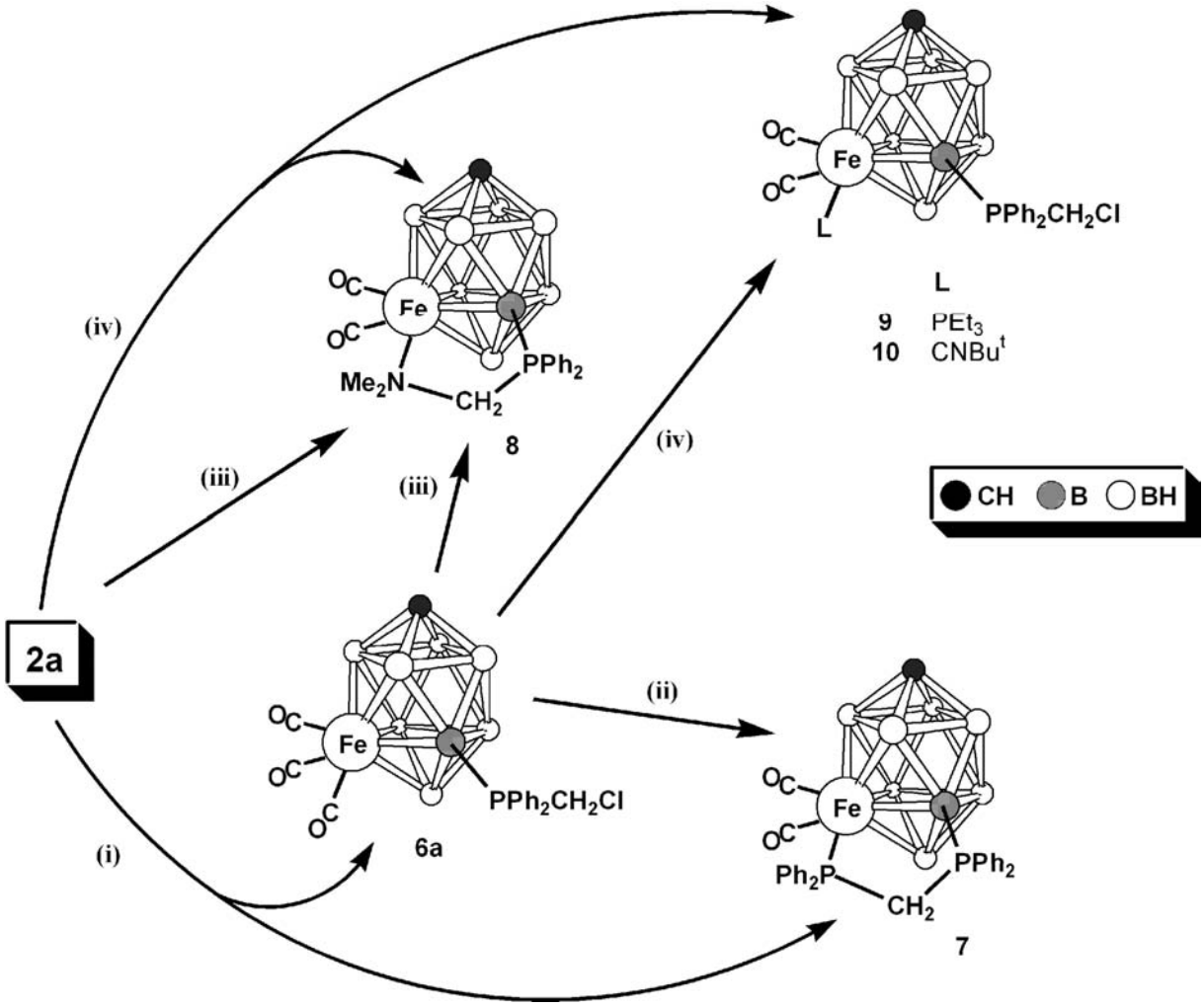

[a] Reagents and conditions: (i) NEt_3 in CH_2Cl_2; (ii) $PHPh_2$ and Me_3NO in CH_2Cl_2; (iii) Me_3NO in CH_2Cl_2; (iv) L and Me_3NO in CH_2Cl_2.

Moreover, the low frequency of the {P−*B*} resonance in the $^{11}B\{^1H\}$ NMR of **6a** would not be expected for a {B−P} vertex occupying a four-connected position. Logically, therefore, the structure shown in Figure 3 is that of **6b**, and supports the formulation for **2b** described previously.

Compound **7** (Scheme 1), which forms as a co-product with **6a** and **6b**, contains a rare example of a B−P−C−P−Fe intramolecular ring. Previous examples of this arrangement are restricted to adducts of the smaller boranes.[13] Although an analogous species derived from **2b** was not observed, its formation cannot be discounted and it may be simply that yields are too low to permit its detection. Spectroscopic data for **7** are listed in Tables 1−3. Two strong CO absorptions are evident at 1994 and 1948 cm^{-1} in the IR spectrum; the $^{13}C\{^1H\}$ NMR spectrum contained two doublet resonances at δ 215.5 [J(PC) = 21 Hz] and δ 212.8 [J(PC) = 19 Hz], indicating as expected unique electronic environments for

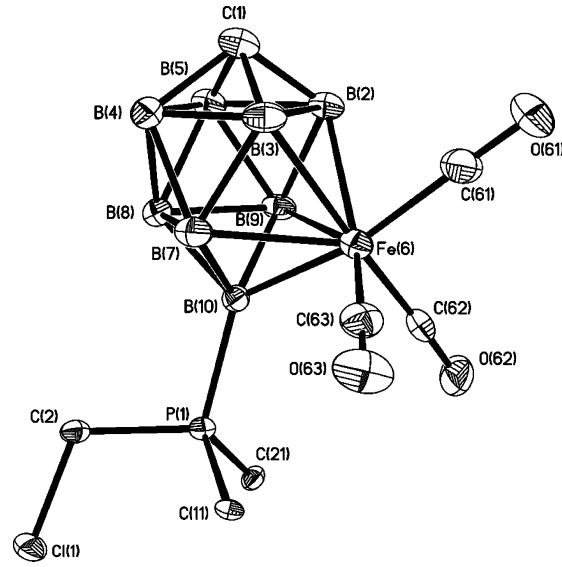

Figure 3. Structure of **6b** showing the crystallographic labeling scheme. Selected distances (Å) are as follows: Fe(6)−B(2) 2.214(5), Fe(6)−B(3) 2.193(5), Fe(6)−B(7) 2.227(5), Fe(6)−B(9) 2.261(5), Fe(6)−B(10) 2.037(4), C(2)−Cl(1) 1.775(4), P(1)−B(10) 1.906(4), P(1)−C(2) 1.825(4).

(13) (a) Alcock, N. W.; Colquhoun, H. M.; Haran, G.; Sawyer, J. F.; Wallbridge, M. G. H. *J. Chem. Soc., Chem. Commun.* **1977**, 368. (b) Alcock, N. W.; Colquhoun, H. M.; Haran, G.; Sawyer, J. F.; Wallbridge, M. G. H. *J. Chem. Soc., Dalton Trans.* **1982**, 2243. (c) Hata, M.; Kawano, Y.; Shimoi, M. *Inorg. Chem.* **1998**, *37*, 4482.

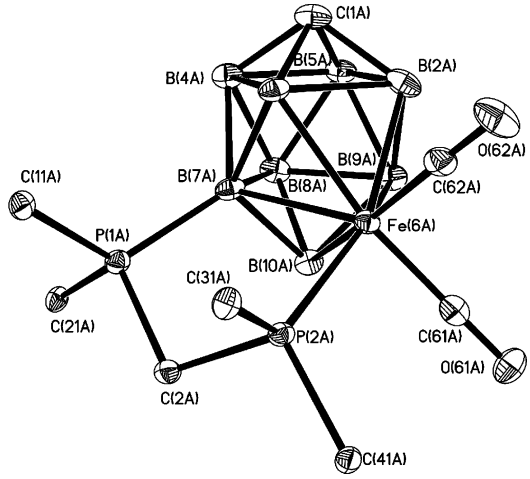

Figure 4. Structure of one of the crystallographically independent molecules of **7** showing the labeling scheme. Selected distances (Å) and angles (deg) are as follows: P(1A)–C(2A) 1.812(3), P(1A)–B(7A) 1.920(4), P(2A)–C(2A) 1.852(3), P(2A)–Fe(6A) 2.2151(8), Fe(6A)–B(7A) 2.189(3); C(2A)–P(1A)–B(7A) 102.76(13), C(2A)–P(2A)–Fe(6A) 110.86(10), P(1A)–C(2A)–P(2A) 107.74(14), B(7A)–Fe(6A)–P(2A) 86.91(9), P(1A)–B(7A)–Fe(6A) 116.20(15).

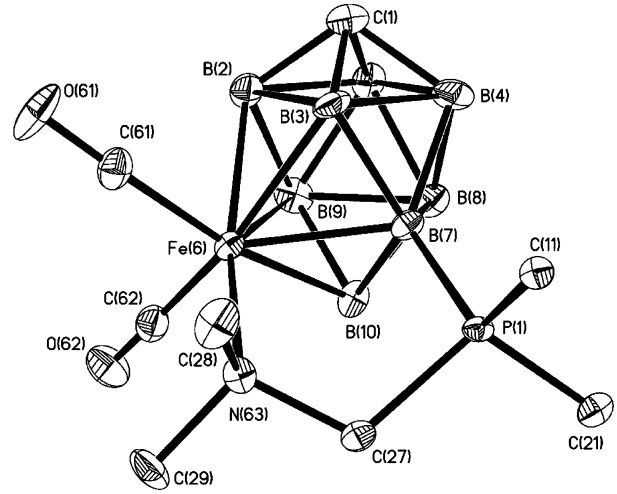

Figure 5. Structure of **8** showing the crystallographic labeling scheme. Selected distances (Å) and angles (deg) are as follows: P(1)−B(7) 1.895(5), P(1)−C(27) 1.814(4), C(27)−N(63) 1.499(5), Fe(6)−N(63) 2.147(3), Fe(6)−B(7) 2.160(5); C(27)−P(1)−B(7) 100.7(2), N(63)−Fe(6)−B(7) 86.91(16), P(1)−B(7)−Fe(6) 110.8(2), N(63)−C(27)−P(1) 111.6(3), C(27)−N(63)−Fe(6) 113.0(2).

the two carbonyl ligands. Resonances due to the cage carbon vertex and to the bridging {PCH_2P} unit were also present at δ 60.7 and 36.7 [dd, J(PC) = 18 and 54 Hz], respectively. The latter moiety gave rise to separate multiplet resonances for each of the two protons in the ^{1}H NMR spectrum. In each case, coupling to the two adjacent phosphorus atoms and the other unique methylene proton resulted in apparent quartet multiplicity. A $^{31}P\{^1H\}$ NMR spectrum revealed a broad multiplet signal centered on δ 18.5 assigned to the {B−P} vertex, in addition to a doublet resonance (δ 77.4) assigned to the {Fe−P} unit [J(PP) = 95 Hz].

One of the crystallographically independent molecules of compound **7** is shown in Figure 4. It is immediately obvious that a carbonyl ligand has been lost from the Fe center and that this has been replaced by the donor phosphorus atom P(2A). With the additional loss of the Cl atom from **6a**, an intermolecular B−P−C−P−Fe ring has been formed. This moiety is puckered, giving an "envelope" conformation, with the {P(1A)C(2A)P(2A)} triangle making an angle of 39.6° with the {P(1A)B(7A)Fe(6A)P(2A)} plane.

The mechanism of formation of **7** is not entirely clear. Perhaps surprisingly, the yield of **7** was not noticeably improved on addition of excess PPh_2Cl to the reaction mixture, suggesting that its formation is associated with decomposition of the precursor **2a** rather than its contamination with traces of this phosphine. Indeed, it seems reasonable that incorporation of $PHPh_2$ by CO substitution of **6a** would be a likely precursor to compound **7**. Thereafter, deprotonation of this Fe-bound $PHPh_2$ ligand, followed by its nucleophilic attack upon the methylene C atom of the PCH_2Cl unit from **6a** would eliminate chloride and form the observed B−PPh_2-CH_2−PPh_2−Fe linkage seen in **7**. In practice, treatment of **6a** in CH_2Cl_2 with $PHPh_2$ and Me_3NO does form small quantities (ca. 10%) of **7**. However, the reaction is complicated by side reactions and the formation of (multiple) other products, including compound **8** described below.

Reaction of **2a** with Me_3NO in the absence of a suitable donor ligand yields the complex [6,6-$(CO)_2$-6,7-μ-{NMe_2-CH_2PPh_2}-*closo*-6,1-$FeCB_8H_8$] (**8**; Scheme 1), which contains an unprecedented intramolecular B−P−C−N−Fe ring. The molecular structure of **8** is presented in Figure 5. In comparison with **2a**, the {*closo*-6,1-$FeCB_8$} unit remains unchanged, but with the five-atom B(7)−P(1)−C(27)−N(63)−Fe(6) ring clearly evident. The latter is puckered, so that the {NCP} triangle makes an angle of 40.8 ° with the {BPNFe} plane.

The IR spectrum of **8** contains strong CO stretching bands at 1983 and 1927 cm^{-1}. In the $^{13}C\{^1H\}$ NMR spectrum two resonances due to these groups were seen at δ 218.2 and 216.4. Peaks due to the cage {CH} (δ 57.9) and NMe_2 groups (δ 62.6 and 60.3) were also present therein, the hydrogen atoms of which gave rise to corresponding peaks in the ^{1}H NMR spectrum at 5.05 (br), and 3.08 and 2.22, respectively. The methylene linkage of the exopolyhedral ring moiety appeared as a doublet resonance [J(PC) = 45 Hz] at δ 68.3 in the $^{13}C\{^1H\}$ spectrum while in the ^{1}H NMR spectrum its two hydrogen atoms gave rise to individual doublet-of-doublet resonances at δ 3.78 [J(PH) = 42 Hz; J(HH) = 13 Hz] and δ 3.15 [J(PH) = 15 Hz; J(HH) = 5 Hz]. The presence of the heteronuclear ring in **8** renders the ferracarborane cluster asymmetric, with eight inequivalent boron atoms, and as such the $^{11}B\{^1H\}$ NMR spectrum contained eight resonances for the boron vertices. Of these, the doublet expected for the {B−P} unit was not clear as that signal coincides with another centered at δ −23.3. However, this moiety is evident in the corresponding $^{31}P\{^1H\}$ NMR spectrum as a quartet at δ 23.7 [J(BP) = 130 Hz].

Compound **8** was also observed as a side-product in reactions intended to produce simple, Fe-substituted derivatives of **2a**. In practice, however, the primary species obtained from such reactions instead were relatives of compound **6a**. Thus, addition of Me_3NO to solutions of **2a** in the presence of ligands L affords [6,6-$(CO)_2$-6-L-7-(PPh_2CH_2Cl)-*closo*-

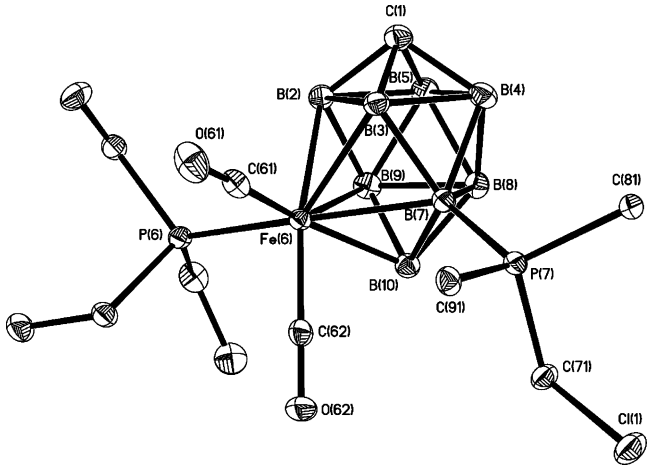

Figure 6. Structure of **9** showing the crystallographic labeling scheme. Selected distances (Å) are as follows: Fe(6)−P(6) 2.2301(5), B(7)−P(7) 1.9178(19), P(7)−C(71) 1.8262(16), C(71)−Cl(1) 1.7824(16), Fe(6)−B(2) 2.2001(18), Fe(6)−B(3) 2.1906(18), Fe(6)−B(7) 2.2131(18), Fe(6)−B(9) 2.2494(19), Fe(6)−B(10), 2.0488(18).

6,1-$FeCB_8H_8$] [L = PEt_3 (**9**) or $CNBu^t$ (**10**)]. In each case, compound **8** is also obtained in significant quantities (Scheme 1). The close similarity of all three species, **6a**, **9**, and **10**, is evident in their near-identical NMR data, save for the additional resonances due to the added ligands L being present in characteristic positions. In particular, the presence of the BP*CH*$_2$*Cl* moiety was immediately noted in the ^{1}H and $^{13}C\{^1H\}$ NMR spectra of **9** and **10**, and the integrity of the B−P linkage was also clear from $^{11}B\{^1H\}$ and $^{31}P\{^1H\}$ NMR spectra. All of this was further substantiated by the molecular structure of **9** established by X-ray diffraction, which is shown in Figure 6. The Fe-bound PEt_3 ligand and the B(7)-bound $\{PPh_2CH_2Cl\}$ unit are clearly evident therein. These data otherwise merit little further comment.

It seems likely the formation of all three of compounds **8**−**10** from **2a** involves compound **6a** as an intermediate. [Indeed, treatment of **6a** with ligands L does indeed form compounds **9** (L = PEt_3) and **10** (L = $CNBu^t$).] We surmise that initial reaction of **2a** with Me_3NO removes a metal-bound CO ligand as CO_2 and liberates Me_3N and that the latter can then convert another molecule of **2a** to **6a** in the same manner as treatment of **2a** with Et_3N discussed above. A straightforward CO → L substitution process then converts **6a** to **9** or **10**, as appropriate. Formation of **8** from **6a** is less well understood. Most probably, **6a** is converted to an Fe-substituted analogue (similar to compounds **9** and **10**) with L = NMe_3, the latter being available in solution as noted above. From there, formal CH_3Cl elimination (from B−PPh_2CH_2−*Cl* and *CH*$_3$−NMe_2−Fe) would afford **8**, a suggestion supported by the fact that compound **8** can be synthesized by direct reaction of **6a** with Me_3NO. Alternatively, an Fe−NMe_3 substituted derivative of **2a** might be invoked, from where formal H_2 elimination (from B−PPh_2−*H* and *H*−CH_2NMe_2−Fe) could also form **8**. Our efforts continue as we seek fully to understand these and related systems.

Conclusions

We have demonstrated a protocol whereby reaction between PPh_2Cl and $Tl[PF_6]$ generates (at least formally) the species $\{PPh_2\}^+$ in situ; the latter then acts as a hydride abstractor toward a {B−H} vertex, forming a molecule of $PHPh_2$ that then binds to the denuded boron atom. Thus, substitution by this phosphine at the B(7) position of the ferracarborane anion in **1** resulted in a metallacarborane containing a $\{B-PHPh_2\}$ vertex (compound **2a**). The acidic nature of the phosphorus-bound hydrogen atom of this group allowed for its removal using a variety of bases, and subsequent derivatization of the phosphine unit. When a pendant propynyl group is introduced at this site, its reaction with $[Co_2(CO)_8]$ afforded a compound containing both a $\{C_2Co_2\}$ tetrahedron and an $\{FeCB_8\}$ cluster linked by a $\{PPh_2\}$ group. Alternatively, deprotonation of the phosphine ligand and addition of a source of $\{Ir(CO)(PPh_3)_2\}^+$ afforded an intramolecular B−P−Ir−B ring. When the deprotonation of the B−$PHPh_2$ ligand in **2a** is performed in the absence of another suitable substrate, reaction with a CH_2Cl_2 solvent molecule instead occurs, affording a $\{B-PPh_2CH_2Cl\}$ vertex. Removal of the chlorine atom of the latter unit is evidently facile and allowed for the preparation of species containing unprecedented 5-membered heteroatomic intramolecular rings.

We believe that the protocol that yielded the parent compounds **2** can likely be extended to substrates other than PPh_2Cl, thus allowing for the introduction of other boron-bound functionalities. Likewise, the possibility (demonstrated herein) of exploiting the acidity of the P−H unit to attach other groups to the cage can be extended in a variety of directions. We are actively exploring all of these avenues.

Experimental Section

General Considerations. All reactions were carried out under an atmosphere of dry, oxygen-free nitrogen using Schlenk-line techniques. Solvents were stored over and freshly distilled from appropriate drying agents prior to use. Petroleum ether refers to that fraction of boiling point 40−60 °C. Chromatography columns (typically ca. 20 cm in length and ca. 2 cm in diameter) were packed with silica gel (Acros, 60−200 mesh). NMR spectra were recorded at the following frequencies: ^{1}H, 360.13; ^{13}C, 90.56; ^{11}B, 115.5; and ^{31}P, 145.78 MHz. Compound **1**[8] and $[IrCl(CO)(PPh_3)_2]$[14] were synthesized as previously described; all other materials were used as received.

Synthesis of [6,6,6-$(CO)_3$-*n*-$(PHPh_2)$-*closo*-6,1-$FeCB_8H_8$] [*n* = 7 (2a), 10 (2b)]. Compound **1** (0.20 g, 0.25 mmol) was dissolved in CH_2Cl_2 (10 mL), and PPh_2Cl (0.1 mL, 0.5 mmol) and $Tl[PF_6]$ (0.18 g, 0.50 mmol) were added. The resulting mixture was stirred for 18 h, volatile material was removed in vacuo and the residue dissolved in CH_2Cl_2/petroleum ether (1:1, 3 mL) before being transferred to the top of a chromatography column. Elution with the same solvent mixture gave a yellow fraction from which removal of solvents yielded yellow microcrystals of **2a** (0.08 g, 72%) that were contaminated with a small amount (<0.005 g) of the isomeric species **2b**.

(14) Vrieze, K.; Collman, J. P.; Sears, C. T.; Kubota, M. *Inorg. Synth.* **1968**, *11*, 101.

Table 4. Crystallographic Data for Compounds **3**, **5**, **6b**, **7**, **8**, and **9**

	3·$2CH_2Cl_2$	**5**	**6b**	**7**·CH_2Cl_2	**8**·CH_2Cl_2	**9**
formula	$C_{54}H_{52}B_8Cl_4FeIrO_4P_3$	$C_{25}H_{21}B_8Co_2FeO_9P$	$C_{17}H_{20}B_8ClFeO_3P$	$C_{29}H_{32}B_8Cl_2FeO_2P_2$	$C_{19}H_{28}B_8Cl_2FeNO_2P$	$C_{22}H_{35}B_8ClFeO_2P_2$
fw	1346.21	756.58	481.08	687.72	546.62	571.22
crystal system	triclinic	monoclinic	monoclinic	monoclinic	orthorhombic	monoclinic
space group	$P\bar{1}$	$P2_1/c$	$P2_1/n$	$P2_1/n$	$Pbca$	$P2_1/n$
a, Å	12.8499(3)	10.9431(10)	10.0669(15)	14.9044(7)	15.2504(17)	14.6201(5)
b, Å	15.1213(4)	25.772(3)	22.458(3)	21.1435(9)	14.8275(17)	11.3672(3)
c, Å	16.2676(4)	12.2708(13)	10.9514(17)	21.6197(10)	23.126(3)	17.1562(6)
α, deg	68.664(1)	90	90	90	90	90
β, deg	77.017(1)	116.374(5)	115.722(2)	103.225(2)	90	103.500(2)
γ, deg	69.987(1)	90	90	90	90	90
V, Å^3	2748.31(12)	3100.5(5)	2230.5(6)	6632.4(5)	5229.5(10)	2772.40(15)
Z	2	4	4	8	8	4
wR_2, R_1 (all data)[a]	0.1488, 0.0782	0.1369, 0.1006	0.1514, 0.1071	0.1077, 0.0640	0.1272, 0.1201	0.0862, 0.0403
wR_2, R_1 (obs[b] data)	0.1340, 0.0554	0.1106, 0.0568	0.1258, 0.0647	0.0963, 0.0433	0.1083, 0.0610	0.0803, 0.0320
GOF[c]	1.033	1.017	1.025	0.990	0.987	1.043

[a] $wR_2 = [\sum\{w(F_o^2 - F_c^2)^2\}/\sum w(F_o^2)^2]^{1/2}$; $R_1 = \sum||F_o| - |F_c||/\sum|F_o|$. [b] $F_o > 4\sigma(F_o)$. [c] GOF $= [\sum\{w(F_o^2 - F_c^2)^2\}/(n-p)]^{1/2}$ where n = number of reflections and p = number of refined parameters.

Synthesis of [6,6,6-(CO)$_3$-4,7-μ-{Ir(H)(CO)(PPh$_3$)$_2$PPh$_2$}-*closo*-6,1-FeCB$_8$H$_7$] (3). A THF solution (20 mL) of **2a** (0.22 g, 0.50 mmol) was treated with NaH (0.16 g, 60% dispersion in mineral oil) and stirred at ambient temperature for 0.25 h. The suspension was then filtered and the filtrate evaporated to dryness in vacuo. The compounds [IrCl(CO)(PPh$_3$)$_2$] (0.39 g, 0.50 mmol), Tl[PF$_6$] (0.17 g, 0.50 mmol), and CH_2Cl_2 (20 mL) were added to the residue and the resulting suspension stirred at room temperature for 18 h. After filtration and evaporation of the resulting filtrate in vacuo, the residue was dissolved in CH_2Cl_2/petroleum ether (1:1, 3 mL), and transferred to the top of a chromatography column. Elution with the same solvent mixture gave a yellow fraction, removal of solvents from which afforded yellow microcrystals of **3** (0.39 g, 61%).

Synthesis of [6,6,6-(CO)$_3$-7-(PPh$_2$C≡CMe)-*closo*-6,1-FeCB$_8$H$_8$] (4). Compound **2a** (0.22 g, 0.50 mmol) was dissolved in CH_2Cl_2 (20 mL). Propargyl bromide (80% solution in toluene, 0.5 mL, 4.5 mmol) and NEt_3 (0.5 mL, 3.6 mmol) were added, and the resulting mixture stirred for 60 h at ambient temperatures. Solvent was removed in vacuo, and the residue dissolved in CH_2Cl_2/petroleum ether (1:1, 3 mL) before being transferred to the top of a chromatography column. Elution with the same solvent mixture gave a yellow fraction, removal of solvents from which afforded yellow microcrystals of **4** (0.17 g, 71%).

Synthesis of [6,6,6-(CO)$_3$-7-(PPh$_2$-{μ-η^2:η^2-C≡CMe)Co$_2$(CO)$_6$})-*closo*-6,1-FeCB$_8$H$_8$] (5). To a CH_2Cl_2 (20 mL) solution of **4** (0.24 g, 0.5 mmol) was added [Co$_2$(CO)$_8$] (0.18 g, 0.51 mmol), and the mixture stirred for 18 h at ambient temperature. Solvents were then removed in vacuo, and the residue dissolved in CH_2Cl_2/petroleum ether (1:1, 3 mL) and subjected to column chromatography. Elution with the same solvent mixture gave a red fraction, which after evaporation yielded red microcrystals of **5** (0.31 g, 82%).

Synthesis of [6,6,6-(CO)$_3$-7-(PPh$_2$CH$_2$Cl)-*closo*-6,1-FeCB$_8$H$_8$] (6a) and [6,6-(CO)$_2$-6,7-μ-{PPh$_2$CH$_2$PPh$_2$}-closo-6,1-FeCB$_8$H$_8$] (7). Compound **2a** (0.22 g, 0.50 mmol) was dissolved in CH_2Cl_2 (20 mL), NEt_3 (0.5 mL, 3.6 mmol) was added, and the mixture stirred for 60 h at ambient temperature. Solvent was removed in vacuo, and the residue redissolved in CH_2Cl_2/petroleum ether (1:1, 3 mL) and applied to a chromatography column. Elution with the same solvent mixture gave a yellow fraction, removal of solvents from which yielded yellow microcrystals of **6a** (0.17 g, 72%). Further elution with CH_2Cl_2/petroleum ether (3:2) gave a second yellow fraction, which afforded yellow microcrystals of **7** (0.04 g, 12%).

Synthesis of [6,6-(CO)$_2$-6,7-μ-{NMe$_2$CH$_2$PPh$_2$}-*closo*-6,1-FeCB$_8$H$_8$] (8). Compound **2a** (0.22 g, 0.50 mmol) was dissolved in CH_2Cl_2 (10 mL), Me_3NO (0.08 g, 1 mmol) was added, and the resulting solution stirred for 60 h at ambient temperature. Solvent was removed under reduced pressure, and the residue dissolved in CH_2Cl_2/petroleum ether (4:1, 3 mL) and applied to a chromatography column. Elution with the same solvent mixture gave an orange fraction, which afforded orange microcrystals of **8** (0.06 g, 26%).

Synthesis of [6,6-(CO)$_2$-6-L-7-(PPh$_2$CH$_2$Cl)-*closo*-6,1-FeCB$_8$H$_8$] [L = PEt$_3$ (9), CNBu^t (10)]. (i) Compound **2a** (0.22 g, 0.50 mmol) was dissolved in CH_2Cl_2 (10 mL), and PEt_3 (0.15 mL, 1.0 mmol) and Me_3NO (0.08 g, 1.0 mmol) were added. The mixture was stirred for 60 h at ambient temperature. Solvent was removed under reduced pressure, and the residue dissolved in CH_2Cl_2/petroleum ether (3:2, 3 mL) and applied to a chromatography column. Elution with the same solvent mixture gave a yellow fraction which, upon removal of solvents, gave yellow microcrystals of **9** (0.15 g, 52%). Further elution with CH_2Cl_2/petroleum ether (4:1) gave an orange fraction, removal of solvents from which yielded orange microcrystals of **8** (0.05 g, 22%).

(ii) Similarly, compound **2a** (0.22 g, 0.50 mmol), CNBu^t (0.11 mL, 1.0 mmol), and Me_3NO (0.08 g, 1.0 mmol) were stirred for 18 h at ambient temperature, with the same workup procedure, yielded yellow microcrystals of **10** (0.15 g, 57%) and orange microcrystals of **8** (ca. 0.04 g, 19%), respectively.

X-ray Diffraction Experiments. Experimental data for compounds **3**, **5**, **6b**, and **7**−**9** are presented in Table 4; those for compound **6a** are included as Supporting Information (see below). Diffraction data were acquired at 110(2) K using a Bruker-Nonius X8 Apex area-detector diffractometer (graphite monochromated Mo Kα radiation, $\lambda = 0.71073$ Å). Several sets of data frames were collected at different θ values for various initial values of ϕ and ω, each frame covering a 0.5° increment of ϕ or ω. The data frames were integrated using SAINT.[15] The substantial redundancy in data allowed empirical absorption corrections (SADABS)[15] to be applied on the basis of multiple measurements of equivalent reflections.

The structures were solved (SHELXS-97)[15] via conventional direct methods and were refined (SHELXL-97) by full-matrix least-squares on all F^2 data using SHELXTL.[15,16] All non-H atoms were assigned anisotropic displacement parameters. The locations of the cage C atoms were verified by examination of the appropriate

(15) *APEX 2*, version 2.1−0; Bruker AXS: Madison, WI, 2003−2004.
(16) *SHELXTL*, version 6.12; Bruker AXS: Madison, WI, 2001.

internuclear distances and the magnitudes of their isotropic thermal displacement parameters. All hydrogen atoms were set riding on their parent atoms in calculated positions and with fixed isotropic thermal parameters [calculated as $U_{iso}(H) = 1.2 \times U_{iso}(parent)$ or $U_{iso}(H) = 1.5 \times U_{iso}(parent)$ for methyl groups], with the exception of the Ir−H which was freely refined.

Compound **3** co-crystallizes with two CH_2Cl_2 solvate molecules in the asymmetric unit. Compound **7** crystallizes with two independent molecules in the unit cell, differing in the relative orientation of a CH_2Cl_2 solvate molecule associated with each. Compound **8** co-crystallizes with one molecule of CH_2Cl_2 in the asymmetric unit.

Acknowledgment. We thank the Robert A. Welch Foundation for support (Grant AA-0006). The Bruker-Nonius X8 APEX diffractometer was purchased with funds received from the National Science Foundation Major Instrumentation Program (Grant CHE-0321214).

Supporting Information Available: Full details of the crystal structure analyses in CIF format, including data for compound **6a**. This material is available free of charge via the Internet at http://pubs.acs.org.

IC800780W